Journal of Materials Science and Engineering A 11 (1-3) (2021) 26-34
doi: 10.17265/2161-6213/2021.1-3.003

Modeling and Simulation of ΔH in Solid State Synthesis of Nanocomposites Al-Cu-Zr

M. Aboelsoud

Physics Dept., The University College in Al-Qunfudah, Umm Al-Qura University, Al Qunfudah 21912, KSA

Abstract: Amorphous structure generated by high-energy ball miller (BM) is often used as a precursor for generating nanocomposites through controlled devitrification. The amorphous forming composition range of ternary Al-Cu-Zr system was calculated using the extended Miedema's semiempirical model. Eleven compositions of Al-Cu-Zr system showed a wide range of negative enthalpy of mixing ($-\Delta H^{mix}$) and amorphization ($-\Delta H^{amor}$) among the constituent elements was selected for synthesis by BM. They yielded either nanocomposites of partial amorphous and crystalline structure or no amorphous phase at all in the as-milled condition. The $Al_{88}Cu_6Zr_6$ alloy with relatively small negative ΔH^{mix} (-0.4 kJ/mol) and ΔH^{amor} (-14.8 kJ/mol) became completely amorphous after 120 h of milling.

Keywords: Al-Cu-Zr nanocomposite materials, high-energy BM, X-ray diffraction (XRD) and transmission electron microscope (TEM), Miedema model analysis.

1. Introduction

An attractive method to produce large quantities of nanostructured composites is the controlled devitrification (crystallization) of amorphous solids [1]. In order to generate the amorphous precursor, mechanical alloying (MA) by high-energy ball milling (BM) of the elemental powder blends is extensively employed as a "far from equilibrium" processing route [1, 2]. When MA is combined with appropriate consolidation techniques, it should be able to circumvent the limitations of melt spinning with respect to restriction in geometry and size of the resulting nanostructured multiphase samples. The former has shown potential in the production of the bulk material without microstructure coarsening, which is typical in cast bulk samples [1]. In the early 1990s, Inoue [3] proposed three empirical rules for the achievement of high amorphous forming ability: (i) negative enthalpy of mixing ($-\Delta H^{mix}$) and amorphization ($-\Delta H^{amor}$) among the constituent elements, (ii) significant difference in atomic size ratio, above 12%, among these elements, and (iii) multicomponent alloy systems consisting of more than three elements. Inoue [3] suggested that a highly negative enthalpy of mixing is more conducive for the amorphous phase formation. Now, due to the increasing interest in the ternary Al-Cu-Zr alloys for structural applications [4-6], this system has been chosen for the present study. Present work attempts to examine, the modeling and simulation of ΔH in solid state synthesis of Al-Cu-Zr nanocomposite materials generated by MA. Comprehensive MA investigations of the corresponding binary systems, i.e. Cu-Al, Cu-Zr, and Al-Zr [7-12] are available to facilitate the study on MA of the Al- Cu-Zr system. Earlier investigations on MA of the ternary Al-Cu-Zr system [13-16] have mainly focused their attention on either Zr-based or Cu-based compositions, apparently because alloys containing more than 80 at.% Al are difficult to amorphize by MA [12, 17, 18].

2. Analytical Model

Miedema's semi-empirical model [19] for binary systems is a very useful tool to calculate the amorphous forming composition range (AFCR),

Corresponding author: M. Aboelsoud, professor, research fields: materials science engineering fields.

where (ΔH^{mix}) is negative. The topic has been extensively reviewed by Weeber and Bakker [20]. The enthalpy of mixing is defined as the difference between the enthalpy of amorphization (ΔH^{amor}) and the enthalpy of solid solution formation (ΔH^{ss}) [21-23]. In the present work, this model has been extended to the ternary system by splitting it to three pseudo-binary systems and neglecting the ternary interaction terms in a manner similar to Bakker et al. [21], Murty et al. [21], and Takeuchi and Inoue [24]. Here the mixing enthalpies of the constituent binary sub-systems as a function of their compositions were calculated on the basis of regular solution model [21]. The neglect of the ternary interaction terms due to the non-availability of related data would certainly introduce some unavoidable error in the enthalpy calculations. The AFCR of the Al-Cu-Zr system at room temperature calculated in this manner is displayed in Fig. 1. The calculated iso-enthalpy contours of ΔH^{amor} for the same system are shown in Fig. 2. These values of enthalpies in Figs. 1 and 2 serve as the basis for selection of the alloy compositions for amorphization, to evaluate the role of ΔH^{mix} and ΔH^{amor}.

3. Experiment

The nominal compositions of the eleven alloys studied in the present investigation are superimposed in Figs. 1 and 2. Elemental blends of these compositions were prepared from Al, Cu and Zr powders (purity ≥ 99.5%) of size 15, 15 and 60 μm, respectively.

MA of these blends was carried out in a high energy Fritsch P5 planetary ball mill, in cemented carbide grinding media at a mill speed of 300 r. p. m. and ball to powder ratio 10:1, using toluene as the process control agent. The identity and phase evolution at different stages of MA were studied by the X-ray diffraction (XRD) analysis of the milled powders using the Co-K_α radiation (λ = 1.78897 nm) in a Philip's X'pert PRO high-resolution X-ray diffractometer. Refined values of lattice parameter (a) were calculated from peak positions in the XRD pattern by extrapolation of a against (cos 2θ⁄sin θ) to cos θ = 0 [25]. The average grain size of Al-rich solid solution was determined from the broadening of a

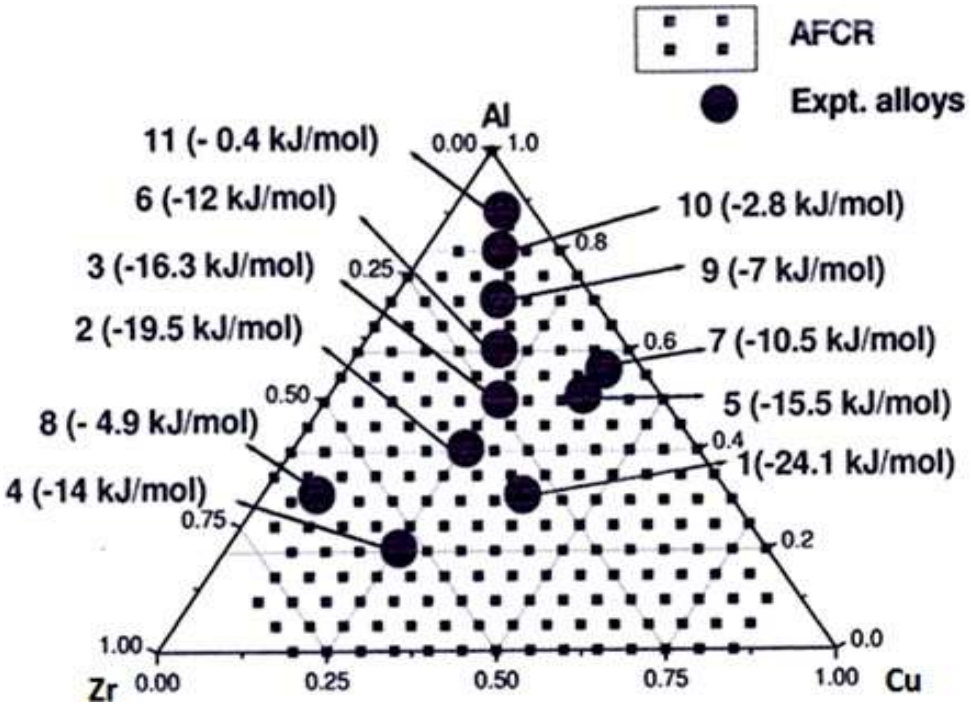

Fig. 1 Amorphous forming composition range (AFCR) of the Al-Cu-Zrsystem, predicted by Miedema's model. Composition of the experimental samples is superimposed; here notations like 5 (-15.5 kJ/mol) indicate alloy 5 having ΔH^{mix} = -15.5kJ/mol.

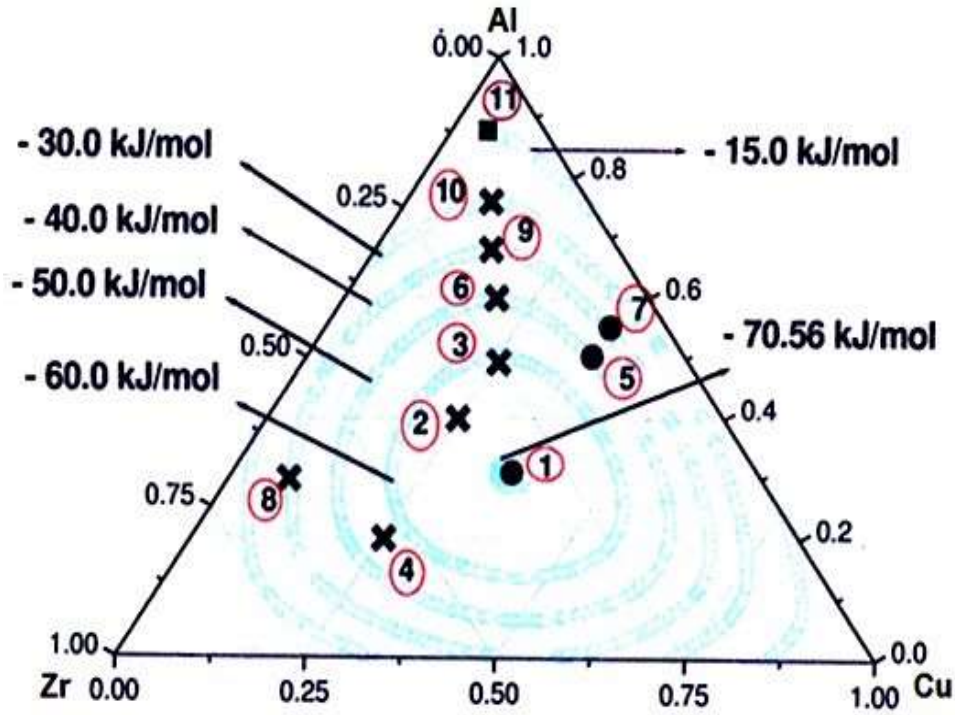

Fig. 2 Plots of calculated iso-enthalpy contours of amorphization (ΔH^{amor}). Experimental alloys selected (e.g. 1, 2, etc.) and the phases evolved in them (e.g. amorphous (■), amorphous plus crystalline (x) and fully crystalline (●)) during MA are also displayed here.

Al_{ddd} reflection after K-α_2 stripping by Philips X'pert Plus software and using Voigt method [26], which allowed judicious elimination of the contribution due to the instrumental and strain effect on the observed peak broadening. For the overlapping peaks, the full width at half intensity maximum and true Bragg angle (2θ) were determined by an appropriate deconvolution exercise. A few samples were examined using JEOL 2000 FX 120 kV transmission electron microscope (TEM).

4. Results

The enthalpies of mixing of the eleven alloys are shown in Fig. 1. The XRD patterns in Fig. 3 show the microstructural evolution during milling of alloy 1 ($Al_{30.5}Cu_{37}Zr_{32.5}$), which has the most negative ΔH^{mix} (-24.1 kJ/mol, Fig. 1) and ΔH^{amor} (-70.6 kJ/mol, Fig. 2).

In course of MA of alloy 1 ($Al_{30.5}Cu_{37}Zr_{32.5}$), the $Al_{0.3}Cu_{0.35}Zr_{32.5}$ intermetallic phase appeared after 10 h of MA, and its amount seemed to increase with the progress of milling, as evidenced by the increase in the relative intensities of the corresponding peaks in Fig. 3. The formation of an amorphous phase was not evident from the XRD patterns at any stage of milling up to 60 h (Fig. 3). Alloy 5 ($Al_{51}Cu_{37}Zr_{12}$) and alloy 7 ($Al_{55.5}Cu_{37}Zr_{7.5}$) showed similar results during their MA, although they were well inside the AFCR (Fig. 1).

The alloy 6 ($Al_{60}Cu_{20}Zr_{20}$) was found to form some amorphous phase along with the crystalline phases of AlCu and Zr_3Al after 10 h of milling as is evident from the XRD patterns in Fig. 4.

The TEM micrograph and selected area diffraction (SAD) pattern of alloy 6 at this stage in Fig. 5 also supported the presence of some amorphous phase along with the crystalline phases. After 20 h of MA the ($Al_{0.3}Cu_{0.35}Zr_{0.35}$) intermetallic phase was detectable and the broad maxima corresponding to the amorphous phase became weaker as compared to that after MA for 10 h (Fig. 4). All the above-mentioned intermetallic phases coexisted in the structure up to 60 h of milling (Fig. 4) indicating their stability in the MA environment.

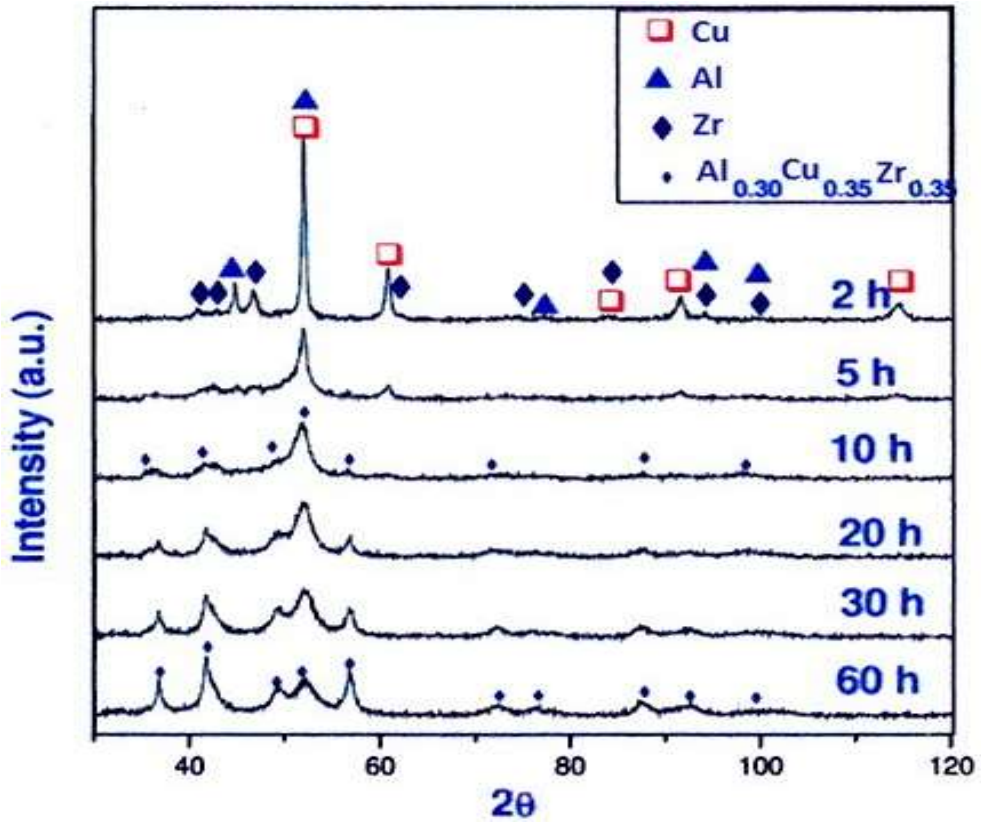

Fig. 3 XRD patterns of alloy 1 ($Al_{30.5}Cu_{37}Zr_{32.5}$) show only crystalline phases even after 60 h of MA.

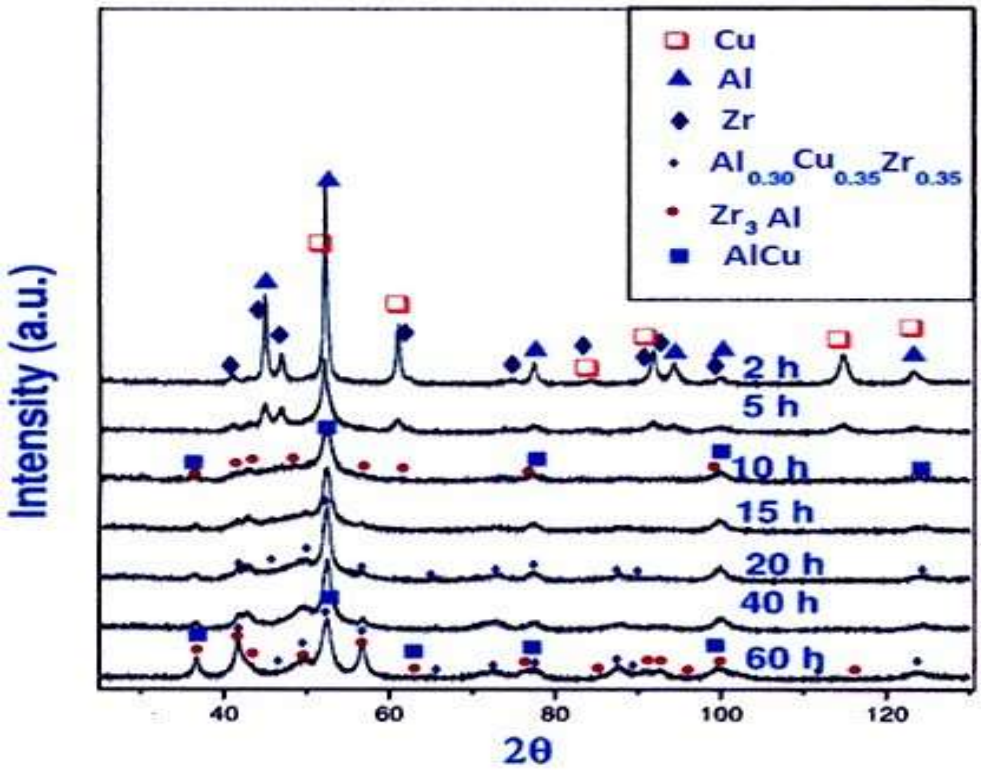

Fig. 4 Modulation of XRD patterns of alloy 6 ($Al_{60}Cu_{20}Zr_{20}$) with milling time. After 10 h of milling, crystalline AlCu phase plus amorphous phase formation is evident. With further increase of milling time the structure becomes fully crystalline.

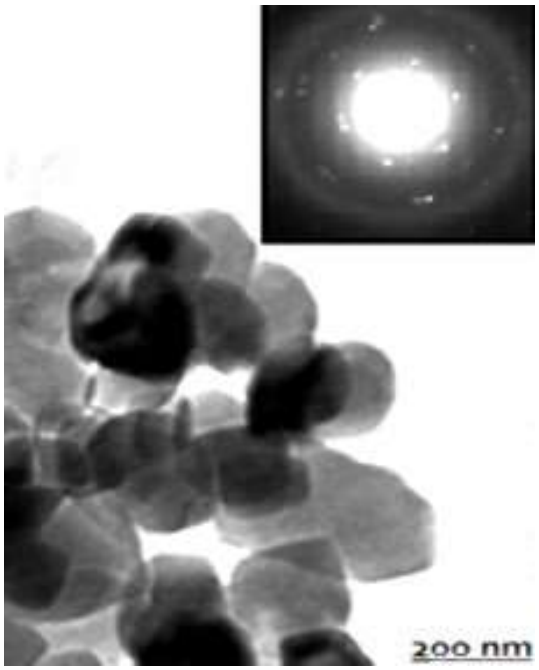

Fig. 5 Transmission electron micrograph of alloy 6 ($Al_{60}Cu_{20}Zr_{20}$) after 10 h of MA. The SAD pattern in the inset shows diffuse ring from amorphous phase and few sharp spots from crystalline phase.

Like alloy 6, the MA of alloy 2 ($Al_{40}Cu_{25}Zr_{35}$), alloy 3 ($Al_{50}Cu_{25}Zr_{25}$), alloy 4 ($Al_{20}Cu_{25}Zr_{55}$), alloy 8 ($Al_{31}Cu_{8}Zr_{61}$), alloy 9 ($Al_{70}Cu_{15}Zr_{15}$) and alloy 10 ($Al_{80}Cu_{10}Zr_{10}$) showed similar trend, i.e. the amorphous plus crystalline phase formed at some intermediate stage of milling, and then on further milling the structure transformed to completely crystalline phase(s). In general, amorphous phase, which forms during non-equilibrium processing (here MA), is a metastable phase, and its further transformation to crystalline phases is possible. Here the presence of the crystalline phase(s) in the amorphous matrix probably provoked this devitrification during further milling. Similar kind of behavior has been reported by Suryanarayana et al. [27] for Zr-Al alloys (Zr—24 at.% Al and Zr—50 at.% Al), Makifuchi et al. [28] for Cu-Zr system and Nagarajan et al. [13] in their study on $Al_{25}Cu_{25}Zr_{50}$ alloy.

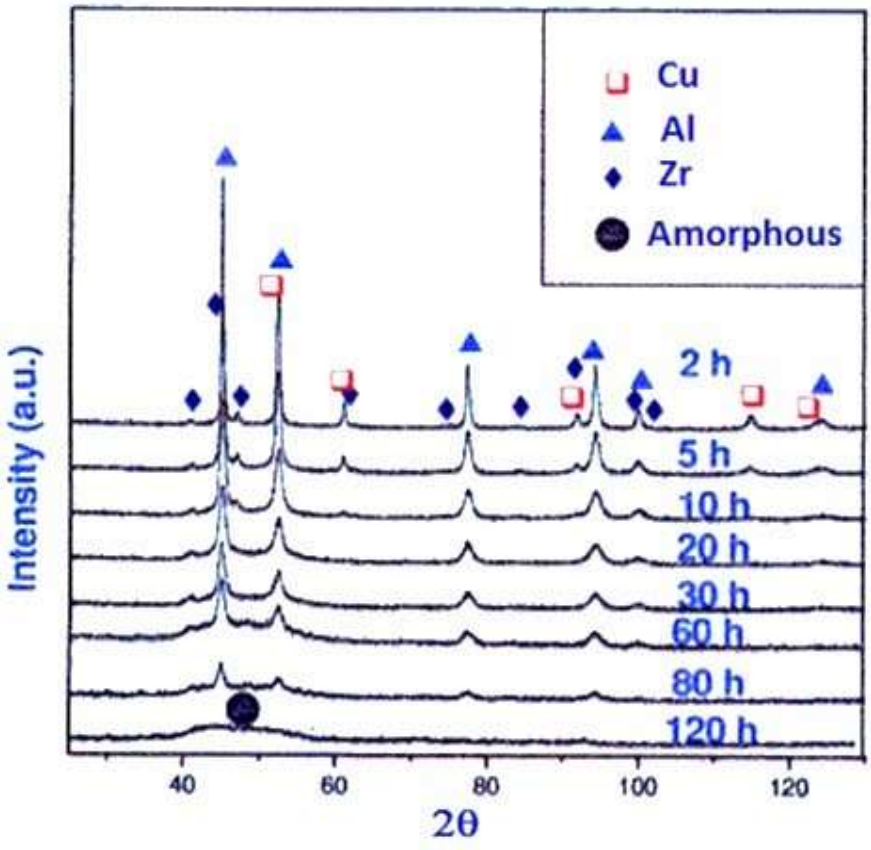

Fig. 6 XRD patterns of alloy 11 ($Al_{88}Cu_{6}Zr_{6}$) evidencing the presence of amorphous phase only after MA for 120 h.

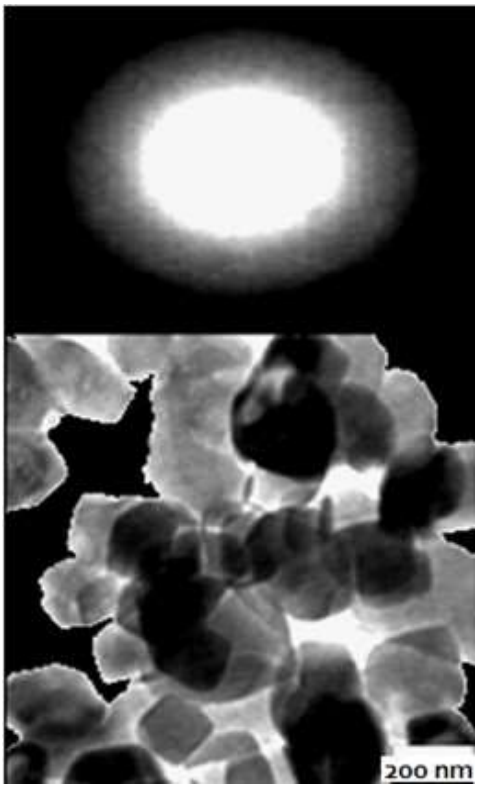

Fig. 7 Transmission electron micrograph of alloy 11 ($Al_{88}Cu_6Zr_6$) after 120 h of MA. The SAD pattern in the inset shows only a diffused ring.

Among all the alloy compositions investigated in the present study, alloy 11 ($Al_{88}Cu_8Zr_6$) lying near the periphery of the AFCR in Fig. 1, and having a very small value of negative enthalpy of mixing (ΔH^{mix} = -0.4 kJ/mol) and amorphization (ΔH^{amor} = -14.8 kJ/mol, Fig. 2) was found to become fully amorphous after 120 h of milling, as evidenced by a broad maxima in the XRD pattern (Fig. 6) and a diffused ring in the SAD pattern in Fig. 7 recorded in the TEM.

An insight into the amorphous phase formation in the alloy 11 during MA can be obtained from the variation of lattice parameter (a_{Al}) and crystallite size of Al with milling time in the alloy 11 (Fig. 8). Here in the early stages of MA from 2 to 5 h, the intensity of Cu peak markedly diminished (Fig. 6) with concurrent reduction in a_{Al} (Fig. 8), which apparently indicated a significant extent of dissolution of Cu in Al after nanocrystallization of Al matrix, because the atomic diameter of Cu (0.249 nm) is smaller than that of Al (0.286 nm). In fact, computer simulation by Basu et al. [29] has earlier shown that nanostructure

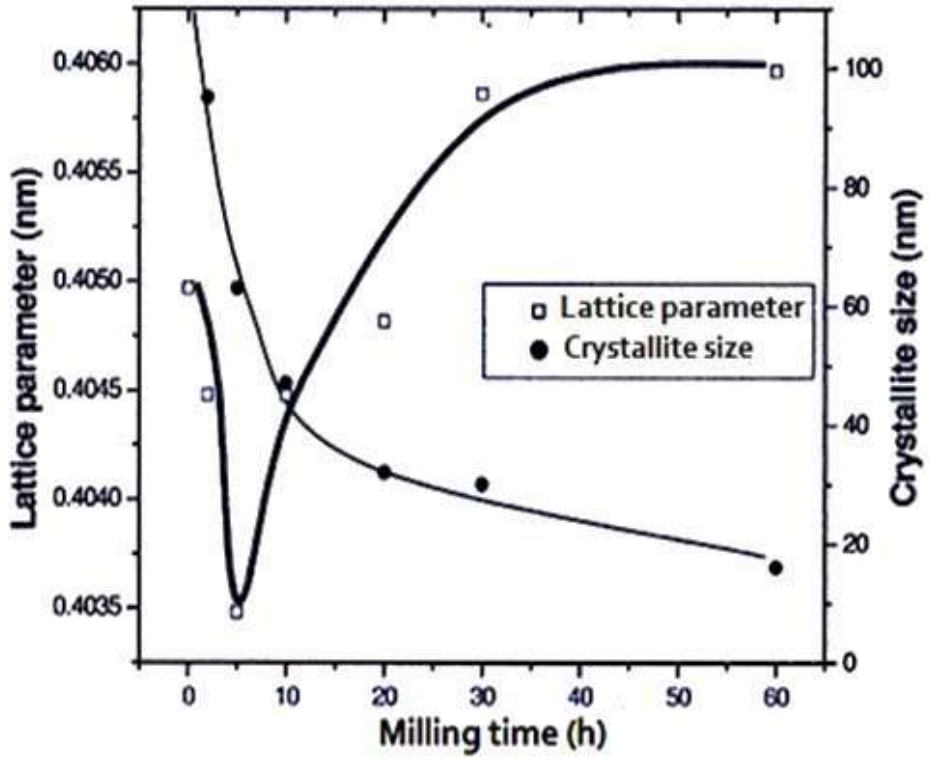

Fig. 8 The variation of crystallite size and lattice parameter of Al during the milling of alloy 11 ($Al_{88}Cu_6Zr_6$).

formation in the MA process is a prerequisite of any significant rate of alloying. When the milling was extended beyond 5 h, a_{Al} decreased (Fig. 8) and relative intensity of the Zr peaks diminished (Fig. 6) up to 30 h of MA, which may be attributed to the dissolution of the larger sized Zr atoms (dia. 0.289 nm) in the Al-rich matrix. The a_{Al} practically remained unchanged beyond 30 h of MA (Fig. 8) apparently indicating the completion of dissolution of Cu and Zr in the Al matrix. Fig. 6 also evidences the presence of some amorphous phase after 30 h of milling. Further milling continued to refine the crystallite size of Al (Fig. 8), and ultimately destabilized the crystalline structure presumably by the accumulation of mechanical disorder in the Al solid solution to yield a completely amorphous structure after 120 h of milling [4, 12, 17] (see Fig. 6).

5. Discussion

Inoue [30] classified the amorphous forming alloys into five groups, namely: (i) ETM-Al-LTM, (ii) LTM-Al-B (or Si), (iii) LTM-ETM-METTALLOID, (iv) LTM-METALLOID, (v) Mg-Ln-LTM and ETM (Zr, Ti)-Be-LTM (LTM: late transition metal and ETM: early transition metal). It is known that complete amorphization is very difficult to achieve during MA of the alloys containing more than 80 at.% Al, and often the structure shows coexistence of an amorphous phase and fcc Al-rich matrix with some intermetallic compound(s) [12, 17, 18]. Schurack et al. [31] reported for the first time complete amorphization in such an Al-based alloy ($Al_{85}Y_8Ni_5Co_2$) with rare-earth element Y [32, 33] by systematic variation and optimization of the milling parameters. To the best of our knowledge, amorphization of $Al_{88}Cu_6Zr_6$ composition is possibly the first report of complete amorphization of a ternary Al-rich (> 80 at.%) Al-ETM-LTM system by MA.

In the present system it was found that amorphous plus some crystalline phases or only crystalline phases formed during MA of the alloys 1-10, which had more negative values of ΔH^{mix} and ΔH^{amor} (Figs. 1 and 2). It is known that the enthalpy of formation of intermetallic compounds is usually much more negative than that for the corresponding amorphous phase formation [19, 29]. But the Miedema's model can not predict the compositions at which such intermetallic phases would form in any given system. In case of MA, the chances of formation of any intermetallic phase(s) utilizing only a part of the constituents and/or the phase evolution sequence can be quite different from that in rapid solidification processing (RSP). This can explain, why the experimentally observed glass-forming compositions in RSP are often different from that for MA [12, 17, 18]. These factors coupled with the simplifications inherent in the present model might have led to the prediction of a wider AFCR compared to that of the experimentally observed model.

In summary, the absolute values of ΔH^{mix} and ΔH^{amor} do not seem to be the appropriate criteria for amorphization in the Al-Cu-Zr system. The kinetic factors like the competition between the amorphization and crystallization, and the structural factors like the extent of the crystallite size refinement and the stability of any intermetallic phase(s) formed during milling under continued deformation may have a decisive role in the amorphization by MA.

6. Conclusion

Complete amorphization by MA could be achieved for the first time in a ternary Al-rich (i.e. > 80 at.% Al) Al-ETM-LTM alloy, namely, $Al_{88}Cu_6Zr_6$. Here the dissolution of Cu and Zr in the Al matrix, coupled with the structural defects induced by the MA process seemed to promote amorphization. In contrast, nanocomposites of amorphous plus crystalline phases formed at intermediate stages of MA in compositions like $Al_{40}Cu_{25}Zr_{35}$, $Al_{50}Cu_{25}Zr_{25}$, $Al_{20}Cu_{25}Zr_{55}$, $Al_{60}Cu_{20}Zr_{20}$, $Al_{31}Cu_8Zr_{61}$, $Al_{70}Cu_{15}Zr_{15}$ and $Al_{80}Cu_{10}Zr_{10}$; but they became fully crystalline on further milling apparently due to the stability of these

intermetallic phases under milling condition. The magnitude of the negative enthalpies of mixing (ΔH^{mix}) and amorphization (ΔH^{amor}) is not reliable for predicting the amorphization in the Al-Cu-Zr system in course of MA.

References

[1] Sordelet, D. J., Rozhkova, E., Besser, M. F., and Kramer, M. J. 2003. "Consolidation of Gas Atomized $Cu_{47}Ti_{34}Zr_{11}Ni_8$ Amorphous Powders." *J. Non- Cryst. Solids* 317: 137-43.

[2] Suryanarayana, C. 1995. "Nanocrystalline Materials." *Int. Mater. Rev.* 40: 41-64.

[3] Inoue, A. 1998. "Amorphous, Nanoquasicrystalline and Nanocrystalline Alloys in Al-Based Systems." *Prog. Mater. Sci.* 43: 365-520.

[4] Yang, R., Leake, J. A., and Cahn, R. W. 1991. "A Microstructural Study of a Ni_2AlTi-Ni(Al, Ti)-Ni_3(Al, Ti) Three-Phase Alloy." *J. Mater. Res.* 6: 343-54.

[5] Naka, S., Thomas, M., and Khan, T. 1992. "Potential and Prospects of Some Intermetallic Compounds for Structural Applications." *Mater. Sci. Tech.* 8: 291-8.

[6] Valiev, R. Z., Islamgaliev, R. K., and Alexandrov, I. V. 2000. "Bulk Nanostructured Materials from Severe Plastic Deformation." *Prog. Mater. Sci.* 45: 103-89.

[7] He, Y., Poon, S. J., and Shiflet, G. J. 1988. "Synthesis and Properties of Metallic Glasses That Contain Aluminum." *Science* 241: 1640-2.

[8] Atzmon, M. 1990. "*In Situ* Thermal Observation of Explosive Compound-Formation Reaction during Mechanical Alloying." *Phys. Rev. Lett.* 64: 487.

[9] Schwarz, R. B., Petrich, R. R., and Saw, C. K. 1985. "The Synthesis of Amorphous Ni-Ti Alloy Powders by Mechanical Alloying." *J. Non-Crvst. Solids* 76: 281-302.

[10] Calin, M., Rudiger, A., and Koester, U. 2000. "Primary Crystallization of Al-Based Metallic Glasses." In *Metastable, Mechanically Alloyed and Nanocrystalline Materials, Pts 1 and 2*. Edited by Eckert, J., Schlorb, H., and Schultz, L. Zurich-Uetikon: Trans Tech Publications Ltd., 359-64.

[11] Guo, W., Martelli, S., Burgio, N., Magini, M., Padella, F., Paradisco, E., and Soletta, I. 1991. "Mechanical Alloying of the Ti-Al System." *J. Mater. Sci.* 24: 6190-6.

[12] Wu, D., Zhang, J., Huang, J. C., Bei, H., and Nieh, T. G. 2001. "Grain-Boundary Strengthening in Nanocrystalline Chromium and the Hall–Petch Coefficient of Body-Centered Cubic Metals." Scripta *Mater.* 68: 118-21.

[13] Nagarajan, R., and Ranganathan, S. 1994. "A Study of the Glass-Forming Range in the Ternary Ti-Ni-Al System by Mechanical Alloying." *Mater. Sci. Eng. A* 179-180: 168-72.

[14] Itzukaichi, T., Umemoto, M., and Cabanas-Moreno, J. G. 1993. "Phases Produced in Mechanically Alloyed Powders of Al-Ni-Ti." *Scripta. Metall. Mater.* 29: 583-8.

[15] Yavari, A. R., Botta Filho, W. J., Rodrigues, C. A. D., Cardoso, K. R., and Valiev, R. 2002. "Nanostructured Bulk $Al_{90}Fe_5Nd_5$ Prepared by Cold Consolidation of Gas Atomised Powder Using Severe Plastic Deformation." *Scripta Mater.* 46: 711-6.

[16] Liu, Z. G., Guo, J. T., and Hu, Z. Q. 1995. "Mechanical Alloying of the Ni-Al (M)(M-Ti, Fe) System." *Mater. Sci. Eng.* 192-193: 577-82.

[17] Inoue, A. 1994. "Fabrication and Novel Properties of Nanostructured Al Base Alloys." *Mater. Sci. Eng. A* 179-180: 57-61.

[18] Benameur, T., Inoue, A., and Masumoto, T. 1994. "Transformation Behavior and Thermal Stability of Al-Based Systems Prepared by Ball Milling." *Nanostruct. Mater.* 4: 303-22.

[19] Boer, F. R., and Perrifor, D. G. 1998. *Cohesion in Metals*. The Netherlands: Elsevier, 1.

[20] Weeber, A. W., and Bakker, H. 1988. "Amorphization by Ball Milling. A Review." *Physica B* 153: 93-135.

[21] Bakker, H., Zhou, G. F., and Yang, H. 1995. "Mechanically Driven Disorder and Phase Transformations in Alloys." *Prog. Mater. Sci.* 39: 241.

[22] Murty, B. S., Ranganathan, S., and Rao, M. M. 1992. "Solid State Amorphization in Binary Ti-Ni, Ti-Cu and Ternary Ti-Ni-Cu System by Mechanical Alloying." *Mater. Sci. Eng. A* 16: 231-40.

[23] Bakker, H. 1998. *Enthalpies in Alloys*. The Netherlands: Trans Tech.

[24] Takeuchi, A., and Inoue, A. 2000. "Calculations of Amorphous-Forming Composition Range for Ternary Alloy Systems and Analyses of Stabilization of Amorphous Phase and Amorphous-Forming Ability." *Mater. Trans.* 42: 1435-44.

[25] Cullity, B. D. 1978. *Elements of X-Ray Diffraction*, 2nd ed. Reading, MA: Addison Wesley, 350.

[26] Robertson, J., Im, J. T., Karaman, I., Hartwig, K. T., and Anderson, I. E. 2003. "Consolidation of Amorphous Copper Based Powder by Equal Channel Angular Extrusion." *J. Non-Cryst. Solids* 317: 144-51.

[27] Suryanarayana, C., Chen, G. H., and Frefer, A. 1992. "Structural Evolution of Mechanically Alloyed Ti-Al Alloys." *Mater. Sci. Eng. A* 158: 93-101.

[28] Makifuchi, Y., Terunuma, Y., and Nagumo, M. 1997. "Structural Relaxation in Amorphous Ni-Ti Alloys Prepared by Mechanical Alloying." *Mater. Sci. Eng. A* 226-228: 312-6.

[29] Basu, J., and Ranganathan, S. 2004. "Crystallisation in

Al-ETM-LTM-La Metallic Glasses." *Intermetallics* 12: 1045-50.

[30] Inoue, A. 2000. "Stabilization of Metallic Supercooled Liquid and Bulk Amorphous Alloys." *Acta Mater.* 48: 279-306.

[31] Schurack, F., Borner, I., Eckert, J., and Schultz, L. 1999. "Synthesis and Properties of Mechanically Alloyed and Ball Milled High Strength Amorphous or Quasicrystalline Al-Alloys." *J. Metastable and Nanocrystalline Mater*. 2: 49.

[32] Gloriant, T., and Greer, A. L. 1998. "Al-Based Nanocrystalline Composites by Rapid Solidification of Al-Ni-Sm Alloys." *Nanostruct. Mater.* 10: 389-96.

[33] Senkov, O. N., Froes, F. H., Stolyarov, V. V., Valiev, R. Z., and Liu, J. 1998. "Microstructure of Aluminum-Iron Alloys Subjected to Severe Plastic Deformation." *Scripta Mater*. 38: 1511-6.